Editors' Suggestion   Featured in Physics

Observation of Mechanical Faraday Effect in Gaseous Media

Alexander A. Milner,[1] Uri Steinitz,[2,3] Ilya Sh. Averbukh,[3] and Valery Milner[1]

[1]*Department of Physics and Astronomy, The University of British Columbia, Vancouver V6T-1Z1, Canada*
[2]*Soreq Nuclear Research Centre, Yavne 8180000, Israel*
[3]*AMOS and Department of Chemical and Biological Physics, The Weizmann Institute of Science, Rehovot 7610001, Israel*

We report the experimental observation of the rotation of the linear polarization of light propagating in a gas of fast-spinning molecules (molecular superrotors). In the observed effect, related to Fermi's prediction of "polarization drag" by a rotating medium, the vector of linear polarization tilts in the direction of molecular rotation. We use an optical centrifuge to bring the molecules in a gas sample to ultrafast unidirectional rotation and measure the polarization drag angles of the order of 10^{-4} rad (with an experimental uncertainty about 10^{-6} rad) over the propagation distance of the order of 1 mm in a number of gases under ambient conditions. We demonstrate an all-optical control of the drag magnitude and direction and investigate the robustness of the mechanical Faraday effect with respect to molecular collisions.

Light interaction with a moving medium intrigued and inspired scientists for a long time [1–4], leading to the creation of the relativity theory. As was demonstrated by Fizeau [2], a moving medium can "drag" light and change its propagation speed. Similarly, when linearly polarized light is transmitted through a rotating dielectric, the polarization plane is slightly rotated, a phenomenon known as polarization drag (or "rotary photon drag"), first studied by Fermi in 1923 [5]. Further studies [6–8] revealed that, in addition to relativistic effects [5], a considerable contribution to the polarization drag comes from the dispersion properties of the medium. Two circularly polarized components of a linearly polarized light experience opposite frequency shifts in the rotating reference frame due to the so-called angular Doppler effect [9]. Optical dispersion causes an accumulated phase lag between them, thus leading to the rotation of the polarization vector. The phenomenon is a mechanical analog of the magnetic Faraday effect associated with the rotation of the polarization plane of light traveling through a medium subject to an external magnetic field and is therefore referred to as "the mechanical Faraday effect" [8,10].

Polarization drag in a rotating solid was first experimentally observed by Jones in a glass sample that was spun to the rotational frequency of up to 140 Hz [11]. That experiment has been a significant tour de force, requiring sensitivity to polarization rotation below 0.1 μrad for detecting the drag angles on the scale of just a few microradians. A related effect was recently reported in [12], where the drag effect was enhanced by many orders of magnitude in a spinning ruby rod due to the resonant interaction, resulting in the extremely slow group velocity of the probe light.

No observation of polarization drag in a gaseous medium has been reported to date, despite the attention it has received in theoretical works [8] and its potentially important role in astrophysical applications [10]. In comparison to solids, the much lower density of gases presents a major challenge for studying this effect in the laboratory. However, a recent proposal for observing the mechanical Faraday effect in gases suggested using the fast unidirectional rotation of individual molecules to compensate for the low sample density [13].

Here, we report on the first experimental demonstration of the mechanical Faraday effect in gases. We optically bring molecules to the state of ultrafast rotation (the so-called superrotor state, SR) by means of a laser tool known as an optical centrifuge [14–17] and measure the induced change in the polarization of a weak probe pulse following the centrifuge excitation.

We observe polarization drag angles on the order of 0.2 mrad for a propagation distance of $l \lesssim 1$ mm in various gases under ambient conditions (O_2, N_2, CO_2, and ambient air) when the maximum rotational frequency of molecules reaches $f_{rot} \sim 6$ THz. These results are in good agreement with the theoretical estimate [13] of the polarization drag angle

$$\Delta\Phi = -\lambda \frac{\partial n}{\partial \lambda} \frac{l}{c} (2\pi f_{rot}) \times P_{SR}, \qquad (1)$$

where c is the speed of light, n is the refractive index, and the dispersion term $-\lambda(\partial n/\partial \lambda) \sim 4 \times 10^{-5}$ for O_2 at standard conditions and the probe wavelength $\lambda \sim 400$ nm [18]. The relative fraction of the centrifuged molecules P_{SR} depends on multiple experimental parameters and is typically on the order of a few percent [19].
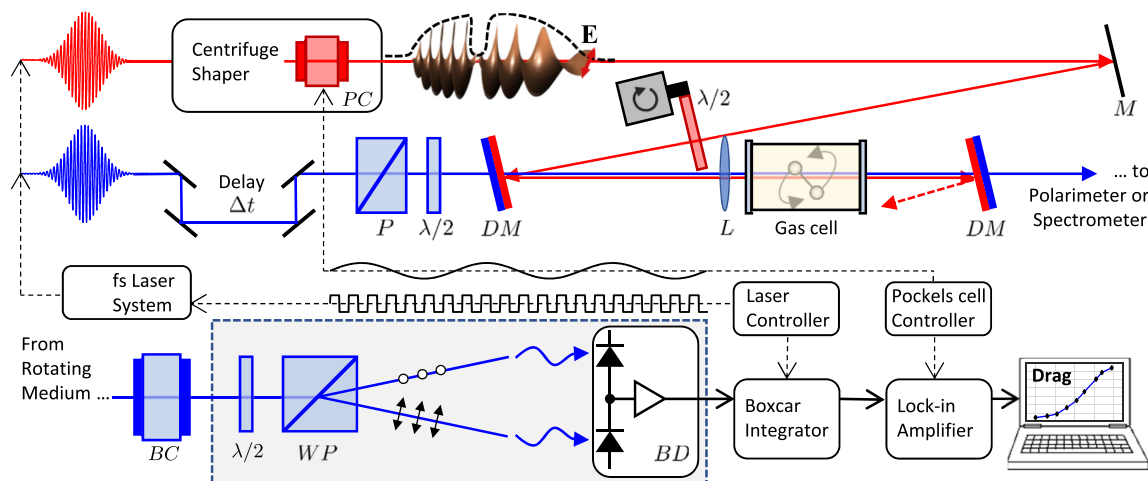
FIG. 1. Scheme of the experimental setup. Top: femtosecond pulses with the central wavelength of 792 nm (upper, red) and 398 nm (lower, blue) are used for creating the centrifuge and the probe pulses, respectively. The pulses are shaped, delayed with respect to one another, combined in a collinear geometry, and focused in a gas cell. Bottom: after passing through the gas sample, probe pulses are filtered out from the centrifuge light and sent to the time-gated polarization analyzer, implemented with a boxcar integrator. PC, Pockels cell; $\lambda/2$, zero-order half wave plate; P, polarizer; M, metallic mirror; DM, dichroic dielectric mirror; L, lens; BC, Berek compensator (Newport 5540); WP, Wollaston prism (Thorlabs WP10-A); BD, balanced detector (Thorlabs PDB220A2). Alternatively, the probe pulses may be sent to a Raman spectrometer to characterize the rotation of the centrifuged molecules.

Remarkably, the specific rotary power (i.e., drag angle per sample density and propagation length) achieved in our experiments is orders of magnitude higher than previously observed in solids [11,12]. In contrast to the slow light experiments [12], where polarization rotation was facilitated by extreme values of the dispersion factor near a narrow optical resonance, here the effect is enhanced by the high frequency of molecular rotation induced by the optical centrifuge. The effect is shown to last on a nanosecond timescale, extending well beyond the centrifuge pulse, until tens of collisions finally cause the molecular superrotors to spin down [20–22]. We also demonstrate optical control of the polarization rotation angle by changing the rotational frequency of the centrifuged molecules.

An optical centrifuge is a laser pulse whose linear polarization rotates with accelerating rate [14,15]. Our setup for producing the centrifuge has been described in a recent review [23]. Briefly, we split the spectrum of broadband laser pulses from a Ti:S amplifier (10 mJ, 35 fs, repetition rate 1 KHz, central wavelength 792 nm) in two equal parts using a Fourier pulse shaper. The two equal-amplitude beams are frequency chirped with opposite chirps and have opposite circular polarizations. When combined together, interference of these laser fields results in the rotation of the polarization vector with a frequency growing linearly in time from 0 to 10 THz over the course of about 100 ps. The centrifuge field interacts with molecules via the induced electric dipole moment. If the interaction potential is strong enough and the acceleration of the centrifuge is not too high, the molecules are excited to high rotational states [23].

The centrifuge pulses are focused in a cell filled with the gas of interest at room temperature and variable pressure, as schematically illustrated in Fig. 1. The focusing lens L with a focal length of 10 cm provides the length of the centrifuged region of about 1 mm and a peak intensity of up to 5×10^{12} W/cm^2. Measuring both the rotational frequency of SRs and the polarization drag angle is accomplished using short probe pulses (pulse lengths of ~ 3 ps) delayed with respect to the centrifuge. The probe pulses are derived from the same laser system, spectrally narrowed to the bandwidth of 0.3 nm and frequency doubled to separate them more easily from the excitation light.

For a given angular acceleration of the centrifuge (here, 0.3 rad/ps^2), the rotational state of the centrifuged molecules is determined by the time of their interaction with the centrifuge field. We vary this time by making a "hole" in the centrifuge pulse at a variable delay from its front edge (see the illustration of a centrifuge pulse at the top of Fig. 1), thus interrupting and effectively terminating the molecular acceleration at any desired rotational frequency [24,25]. We use coherent Raman spectroscopy to characterize molecular rotation, both in terms of its frequency and sense. Coherent scattering of narrow band probe pulses from aligned rotating O$_2$ molecules results in Raman spectra with well-resolved peaks, corresponding to individual rotational quantum states, as described in Sec. S1 of the Supplemental Material [25]. The magnitude of the Raman shift is translated to the rotational frequency, whereas its sign indicates the sense of rotation with respect to the circular probe polarization [26,27].

Our method of detecting a small degree of polarization rotation is based on an optical configuration depicted in the dashed gray rectangle at the bottom of Fig. 1. A half wave plate is used to align the probe polarization at 45° with respect to the axes of a Wollaston prism. This equalizes the intensity of light in both arms of a differential balanced detector, resulting in a zero signal. As soon as the probe polarization undergoes rotation in the sample medium, the balance shifts toward one of the photodiodes yielding a signal, whose sign indicates the direction of rotation. Calibration is achieved via the rotation of the input polarization by a known amount using the same half wave plate.

Because of the short lifetime of the molecular rotation under ambient conditions (nanosecond timescale), we use picosecond probe pulses (same pulses as in the Raman scattering experiment, but linearly polarized) to measure the polarization rotation angle at a given time delay. Signals from the amplified balanced detectors are gated around the arrival time of the probe pulses with a boxcar integrator. To increase our detection sensitivity, we modulate the sense of the centrifuge rotation between clockwise (CW) and counterclockwise (CCW) by means of a Pockels cell and amplified the polarization drag signal at the modulation frequency of $f_{\mathrm{mod}} = 37$ Hz using a lock-in amplifier (see details in Sec. S2 of the Supplemental Material [25]).

Detection of the polarization drag in any media is susceptible to the *linear* birefringence (LB), which may be created in the sample due to its forced rotation. Similar to the mechanical Faraday effect, LB also changes the polarization axes and may completely overwhelm and mask the more subtle drag effect. In the case of a gas sample, LB stems from the anisotropic spatial distribution of the molecular axes during the period of the laser-driven molecular rotation, known as molecular alignment [28–30]. When produced by a short linearly polarized pulse, such an anisotropy results in a refractive index difference for the probe field polarized along and perpendicular to the alignment axis on the order of $n_{\parallel} - n_{\perp} \approx 10^{-5}$ [31,32]. Linear birefringence of this magnitude (hereafter referred to as $\mathrm{LB}_{\mathrm{rot}}$) would yield a half wave retardance for a probe wavelength of 400 nm over a distance of 2 cm, completely changing its polarization direction.

Because the polarization vector of an optical centrifuge $\hat{e}_{\mathrm{cfg}}(t)$ completes up to 500 full rotations, one could naïvely expect that it induces no linear birefringence with a fixed preferential anisotropy axis. Unfortunately, the nonadiabatic front edge of the centrifuge acts similar to a short pulse, creating a small degree of alignment and, correspondingly, a nonzero $\mathrm{LB}_{\mathrm{rot}}$ in the rotating ensemble. Being the result of an optical interference between the two centrifuge arms, the orientation of the linear polarization of the front edge $\hat{e}_{\mathrm{cfg}}(0)$ is changing randomly on a wide range of timescales, introducing large unpredictable fluctuations in the measured drag signal.

To eliminate this artifact, we insert in the path of the centrifuge beam an additional half wave plate, mounted on a motorized rotational stage (a box labeled with "↻" in Fig. 1), and rotate the wave plate continuously with the frequency of $f_{\lambda/2} \approx 10$ rev/s. This half wave plate randomizes the orientation of the polarization vector at the front edge of the centrifuge, since it depends on the relative angle between $\hat{e}_{\mathrm{cfg}}(0)$ and the instantaneous orientation of the rotating axes of the plate at the arrival time of the pulse [33]. Our numerical analysis, described in detail in Sec. S3 of the Supplemental Material [25], shows that the plate's rotation results in the oscillations of the drag signal *around* its true value with the frequency $2f_{\lambda/2}$ and an amplitude proportional to both $\mathrm{LB}_{\mathrm{rot}}$ and the combined static birefringence of all-optical elements. We minimize the latter by means of a Berek compensator to improve the sensitivity of the lock-in detection to the centrifuge modulation frequency f_{mod}. Averaging the lock-in signal over the rotation period of the half wave plate results in an almost complete cancellation of the random error related to $\mathrm{LB}_{\mathrm{rot}}$.

Measuring the polarization drag in gases also suffers from a systematic error related to the collision-induced decay of the unidirectional molecular rotation and the subsequent rotational energy transfer to heat. This leads to the formation of refractive "density depression channels" [21,22,34–36], capable of shifting the position of the probe beam with respect to both the centrifuged molecules and the photodetector. Given that the CW and CCW centrifuges may create slightly different refractive channels (e.g., due to the Pockels cell-induced movement of the centrifuge beam), the effect will generate a nonzero response at the modulation frequency f_{mod}, contaminating the polarization drag signal. To cancel out this artifact, we perform every measurement at two orthogonal polarizations of the probe pulses. Mechanical Faraday rotation will either increase or decrease the projection of the probe polarization on one of the Wollaston axes, depending on whether their initial relative angle is +45° or −45°. Hence, flipping the probe polarization by 90° results in the sign reversal of the drag signal. On the other hand, polarization-insensitive refractive effects remain constant and can therefore be eliminated by calculating the half-difference of the results of the two measurements.

The developed experimental procedure enables us to detect the rotation-induced polarization drag in gases, despite the significantly lower density of gaseous media and a much shorter effective optical length, as compared to previous experiments with rotating solids [11,12]. As shown in Fig. 2, shortly after the end of the centrifuge pulse we observe polarization drag angles on the order of 200 μrad in oxygen, centrifuged to $f_{\mathrm{rot}} \sim 6$ THz, under ambient conditions. Lowering the pressure by a factor of 2 results in a similar drop in the drag signal, as expected from the linear scaling with the number density of the superrotors [13].
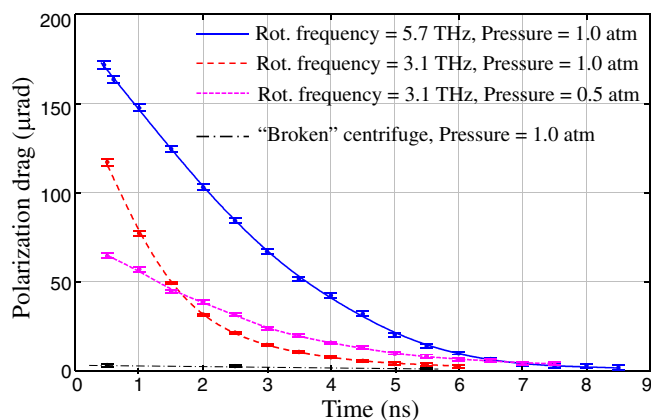
FIG. 2. Experimentally measured decay of the polarization drag signal for two rotational frequencies of oxygen superrotors and two gas pressures. Cubic splines are drawn through the corresponding data points for guiding the eye. A "broken" centrifuge does not produce any molecular superrotors (see text for details). Vertical error bars represent the standard error of the mean over $\sim 10^5$ laser pulses.
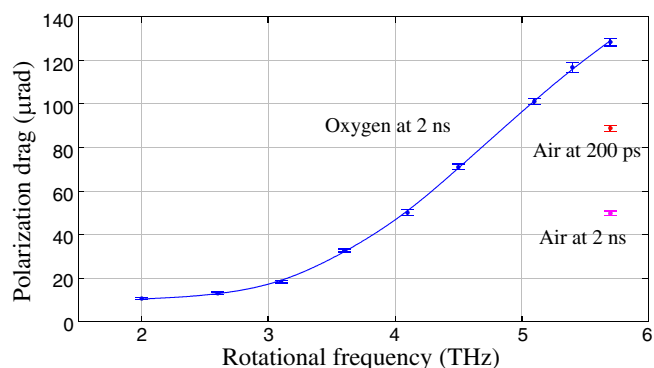

FIG. 3. Experimentally measured dependence of the polarization drag signal on the initial rotational frequency of oxygen superrotors 2 ns after their release from an optical centrifuge (blue dots, connected by the cubic spline to guide the eye). The red and magenta dots correspond to the drag signal in ambient air 200 ps and 2 ns after the centrifuge, respectively. Vertical error bars represent the standard error of the mean over $\sim 10^5$ laser pulses.

As superrotors collide, their rotational frequency decreases, causing the observable polarization drag to decay. At the higher frequency of 5.7 THz (solid blue curve in Fig. 2), the characteristic $(1/e)$ decay time of ~ 3 ns is consistent with what we have found in our earlier work on the collision-induced rotational relaxation in the gas of molecular superrotors [21]. Lowering the rotational frequency to 3.1 THz (dashed red curve) results in a shorter decay time of ~ 1 ns, as anticipated from the faster collisional relaxation at lower levels of rotational excitation [37,38]. Reducing the gas pressure from 1.0 to 0.5 atm changes the decay constant from ~ 1 to ~ 2 ns due to the increased time between collisions.

Note that the evolution of the rotational distribution of centrifuged molecules in time is rather complex. At relatively short delays of $\lesssim 0.5$ ns after the centrifuge pulse, it consists of both the slow and fast molecular rotors (for details, see Sec. S1 of the Supplemental Material [25]), whose collisional relaxation dynamics are very different [20,22]. We therefore expect an equally complex behavior of the polarization drag signal, especially at short delays, exhibiting a nonexponential decay as well as a nonlinear relation between the drag angles and the initial rotational frequency or gas pressure, as indeed found in this Letter (cf. signal magnitudes at 500 ps, 1 atm, and rotational frequencies of 3.1 vs 5.7 THz).

To verify the rotational mechanism of the observed mechanical Faraday effect, we modify the field of an optical centrifuge to start its rotation at a relatively high frequency of 2 THz. Because of such a fast start, this broken centrifuge is incapable of adiabatically trapping the molecules at the beginning of the pulse and spinning them to high rotational states, despite carrying 82% of its initial energy. Very low drag signals, measured at 0.5, 2.5,

and 5.5 ns, and shown by the dash-dotted black line in Fig. 2, confirm the direct connection between the mechanical Faraday effect and the unidirectional molecular rotation. The nonzero residual signal is likely due to the small number of superrotors created by the broken centrifuge.

A more detailed study of the mechanical Faraday effect as a function of the frequency of unidirectional molecular rotation is shown in Fig. 3. Measured in oxygen under the pressure of 1 atm at a time delay of 2 ns after the centrifuge, the polarization rotation angle grows from 0 to 130 μrad with the increase of rotational frequency. We attribute a somewhat larger value at 5.7 THz than in Fig. 2 to the higher capture efficiency of the centrifuge, which is hard to reproduce from one experiment to the other. The superlinear growth stems from the longer lifetime of faster superrotors compared to the slower ones. Hence, higher rotational frequencies increase both the density of molecules remaining in unidirectional rotation (since faster rotors are less susceptible to the collisional decay) and the amount of polarization drag per molecule.

In summary, we report the first experimental observation of the mechanical Faraday effect (also known as rotary polarization drag) in gaseous media. The effect, previously observed only in rotating solids, became accessible in a gas sample due to the high frequency of molecular spinning (≈ 6 THz) induced and controlled by an optical centrifuge. Rotating oxygen molecules drag the linear polarization of a weak probe light by an angle of up to 180 μrad in the direction of their rotation. Polarization drag of comparable magnitude was also observed in ambient air (see Fig. 3), as well as in N_2 and CO_2 samples. The dependence of the observed centrifuge-induced mechanical Faraday rotation on time and rotational frequency is in good qualitative agreement with the

theoretically expected behavior. The nonresonant nature of the effect and its robustness with respect to collisions means that it can be studied in other gases and under various conditions. Producing an equivalent magneto-optic Faraday effect in these gases would require an immense magnetic field of $\sim 50\,T$ [39].

The developed time-resolved polarimetry technique may be useful in probing the dynamics of superrotors, such as their gyroscopic stability followed by an explosive collisional relaxation [20,22], as well as in the studies of polarization rotation in chiral molecules and its relation to their interaction with an optical centrifuge [40,41]. Here, the revealed sensitivity of the apparent drag angle to minute amounts of linear birefringence, inevitably induced in gas samples by strong polarized laser pulses, must be considered carefully. The demonstrated method of examination and cancellation of birefringence-related errors should be useful in future experiments on light propagation in gaseous media interacting with strong polarized optical fields.

[1] A. J. Fresnel, Ann. Chem. Phys. **9**, 57 (1818).

[2] A.-H. Fizeau, C.R. Hebd. Séances Acad. Sci. **33**, 349 (1851).

[3] J. J. Thomson, Proc. Cambridge Philos. Soc. **5**, 250 (1885).

[4] A. A. Michelson and E. W. Morley, Am. J. Sci. **s3-34**, 333 (1887).

[5] E. Fermi, Rend. Lincei Sci. Fis. Nat. **32**, 115 (1923).

[6] M. A. Player and R. V. Jones, Proc. R. Soc. A **349**, 441 (1976).

[7] M. W. Evans, Int. J. Mod. Phys. B **06**, 3043 (1992).

[8] G. Nienhuis, J. P. Woerdman, and I. Kuščer, Phys. Rev. A **46**, 7079 (1992).

[9] B. A. Garetz, J. Opt. Soc. Am. **71**, 609 (1981).

[10] R. Gueroult, Y. Shi, J.-M. Rax, and N. J. Fisch, Nat. Commun. **10**, 3232 (2019).

[11] R. V. Jones, Proc. R. Soc. A **349**, 423 (1976).

[12] S. Franke-Arnold, G. Gibson, R. W. Boyd, and M. J. Padgett, Science **333**, 65 (2011).

[13] U. Steinitz and I. Sh. Averbukh, Phys. Rev. A **101**, 021404(R) (2020).

[14] J. Karczmarek, J. Wright, P. Corkum, and M. Ivanov, Phys. Rev. Lett. **82**, 3420 (1999).

[15] D. M. Villeneuve, S. A. Aseyev, P. Dietrich, M. Spanner, M. Y. Ivanov, and P. B. Corkum, Phys. Rev. Lett. **85**, 542 (2000).

[16] L. Yuan, S. W. Teitelbaum, A. Robinson, and A. S. Mullin, Proc. Natl. Acad. Sci. U.S.A. **108**, 6872 (2011).

[17] A. Korobenko, A. A. Milner, and V. Milner, Phys. Rev. Lett. **112**, 113004 (2014).

[18] P. Křen, Appl. Opt. **50**, 6484 (2011).

[19] J. Floß, C. Boulet, J.-M. Hartmann, A. A. Milner, and V. Milner, Phys. Rev. A **98**, 043401 (2018).

[20] Y. Khodorkovsky, U. Steinitz, J.-M. Hartmann, and I. Sh. Averbukh, Nat. Commun. **6**, 7791 (2015).

[21] A. A. Milner, A. Korobenko, K. Rezaiezadeh, and V. Milner, Phys. Rev. X **5**, 031041 (2015).

[22] U. Steinitz, Y. Khodorkovsky, J.-M. Hartmann, and I. Sh. Averbukh, ChemPhysChem **17**, 3795 (2016).

[23] I. MacPhail-Bartley, W. W. Wasserman, A. A. Milner, and V. Milner, Rev. Sci. Instrum. **91**, 045122 (2020).

[24] P. Amani, A. A. Milner, and V. Milner, arXiv:2106.12468.

[25] See Supplemental Material at http://link.aps.org/supplemental/10.1103/PhysRevLett.127.073901 for technical details on the preparation of molecular superrotors, the method of modulating the sense of their rotation, and the technique of eliminating the effect of the laser-induced linear birefringence on the polarization drag signal.

[26] O. Korech, U. Steinitz, R. J. Gordon, I. Sh. Averbukh, and Y. Prior, Nat. Photonics **7**, 711 (2013).

[27] A. Korobenko, A. A. Milner, and V. Milner, Phys. Rev. Lett. **112**, 113004 (2014).

[28] H. Stapelfeldt and T. Seideman, Rev. Mod. Phys. **75**, 543 (2003).

[29] Y. Ohshima and H. Hasegawa, Int. Rev. Phys. Chem. **29**, 619 (2010).

[30] S. Fleischer, Y. Khodorkovsky, E. Gershnabel, Y. Prior, and I. Sh. Averbukh, Isr. J. Chem. **52**, 414 (2012).

[31] V. Renard, M. Renard, S. Guérin, Y. T. Pashayan, B. Lavorel, O. Faucher, and H. R. Jauslin, Phys. Rev. Lett. **90**, 153601 (2003).

[32] V. Renard, M. Renard, A. Rouzée, S. Guérin, H. R. Jauslin, B. Lavorel, and O. Faucher, Phys. Rev. A **70**, 033420 (2004).

[33] The half wave plate also reverses the sense of the centrifuge rotation, CW⇆CCW, which is taken into account in our data analysis.

[34] U. Steinitz, Y. Prior, and I. Sh. Averbukh, Phys. Rev. Lett. **109**, 033001 (2012).

[35] N. Jhajj, E. W. Rosenthal, R. Birnbaum, J. K. Wahlstrand, and H. M. Milchberg, Phys. Rev. X **4**, 011027 (2014).

[36] O. Lahav, L. Levi, I. Orr, R. A. Nemirovsky, J. Nemirovsky, I. Kaminer, M. Segev, and O. Cohen, Phys. Rev. A **90**, 021801(R) (2014).

[37] J.-M. Hartmann and C. Boulet, J. Chem. Phys. **136**, 184302 (2012).

[38] A. A. Milner, A. Korobenko, J. W. Hepburn, and V. Milner, Phys. Rev. Lett. **113**, 043005 (2014).

[39] L. Ingersoll and D. Liebenberg, J. Opt. Soc. Am. **44**, 566 (1954).

[40] I. Tutunnikov, E. Gershnabel, S. Gold, and I. Sh. Averbukh, J. Phys. Chem. Lett. **9**, 1105 (2018).

[41] A. A. Milner, J. A. M. Fordyce, I. MacPhail-Bartley, W. Wasserman, V. Milner, I. Tutunnikov, and I. Sh. Averbukh, Phys. Rev. Lett. **122**, 223201 (2019).